J. RADIAT. RES., 44, 345–352 (2003) http://jrr.jstage.jst.go.jp

Neuropathology of Delayed Encephalopathy in Cats Induced by Heavy-ion Irradiation

RIKI OKEDA[1], SHINOBU OKADA[2], AKIHIRO KAWANO[3], SATORU MATSUSHITA[4] and TOSHIHIKO KUROIWA[1]*

Heavy-ion irradiation/Delayed encephalopathy/Delayed myelopathy/Brain edema/Hyperpermeability.

Aim: The pathogenesis of delayed encephalopathy induced by heavy-ion irradiation was investigated experimentally in cats. The left cerebral hemispheres were irradiated with 15–40 Gy of heavy ions (carbon), and histologically and morphometrically examined 12 months later. Results: In the irradiated cerebral white matter the following occurred as the dose increased: astrocytic swelling, then the dilatation of small blood vessels with a fibrous thickening of the wall, and then loosening of the white matter with cavity formation and diffuse albumin deposition. Pathological features of these cavities suggested that they are induced by long-standing edema. Although the dilated vessels were arteries, veins, and capillaries, arteriovenous shunt and damage of the smooth muscle cells of the arterial media were absent. Changes of the cerebral cortex were scarce. Morphometrically, the irradiated cerebral white matter was swollen, and the capillary density tended to be reduced in the deep cortex and subcortical white matter, but this effect was not dose dependent. Conclusion: Heavy-ion irradiation induces delayed encephalopathy in cats, preferentially involving the white matter. The cardinal pathogenesis was long-standing edema of the white matter due to vascular hyperpermeability, and the vascular dilatation seemed to be caused by a reduction in the vascular bed and/or hemoconcentration due to hyperpermeability.

INTRODUCTION

There is still controversy between vascular and glial pathogeneses of delayed injury of the central nervous system (CNS) induced by radiation, although the former theory predominates from the numerous experimental and clinicopathological studies that have been reported. Recently, heavy-ion irradiation has been adopted as an alternative to X-ray radiotherapy for cancer. Heavy-ion irradiation has a higher linear energy transfer (LET) than X-rays, and exhibits a Bragg-peak effect that causes the energy to be released explosively at a certain skin depth. This makes heavy-ion irradiation a particularly suitable cancer therapy, because a restricted region can be selectively irradiated with a massive dose using appropriate filters without significant damage to the surrounding normal tissue. However, it is imperative to investigate the nature and pathogenesis of normal CNS tissue damage by heavy-ion irradiation, especially compared to that by X-rays. Our previous experiments into heavy-ion-induced myelopathy in rats showed that the heavy-ion irradiation induces delayed destructive injury similar to that induced by X-ray irradiation, and that the effective dose to induce 50% incidence (ED_{50}) of hind-limb paralysis and destructive cavity formation was lower and the latent period was shorter than those for X-ray irradiation.[1,2)] Moreover, it was elucidated that the delayed destruction of the parenchyma, which was preferentially localized in the bilateral lateral funiculus, is initiated by severe edema around small veins from 16 weeks after irradiation, as is the case for X-ray irradiation. However, the disturbance of the blood–brain barrier, as examined immunohistochemically by an endothelial barrier antigen (EBA), was not restricted in the lateral funiculus, but occurred diffusely in the irradiated white matter of the spinal cord.[3)] These observations of a preferential involvement of the lateral funiculus in X-ray and heavy-ion irradiation are probably due to an anatomical specificity of the venous system of the rat spinal cord: venous stagnation tends to occur in the lateral funiculus because it is located furthest from the venous drainage point along the anterior and posterior roots; this feature is common to the human spinal cord.

*Corresponding author: Phone/Fax: +81-3-5803-5848,
E-mail: t.kuroiwa.npat@mri.tmd.ac.jp
[1]Department of Neuropathology, Medical Research Institute, Tokyo Medical & Dental University, Tokyo, Japan; [2]Department of Pathobiology, School of Nursing, Chiba University, Chiba, Japan; [3]Laboratory Animal Development Section, Department of Technical Support and Development, National Institute of Radiological Sciences, Chiba, Japan; [4]Laboratory Animal Development and Research Group, Research Center for Radiation Safety, National Institute of Radiological Sciences, Chiba, Japan.

The aim of this study was to analyze the pathogenesis of delayed encephalopathy induced by heavy-ion irradiation in cats by (1) comparing it with that of heavy-ion-induced myelopathy in rats, (2) investigating histologically the vascular changes and the spatial relationship between the parenchymal injury and vessels in the irradiated cerebrum by reconstruction of serial sections, and (3) investigating morphometrically the changes in the capillary density and volume of the irradiated cortex and white matter. Cats were used because the encephalopathy induced by X-ray irradiation in animals and humans occurs preferentially in the white matter, which is considerably more developed in cats than in rodents.

MATERIALS AND METHODS

Nine adult male cats (domesticated feline (felis catus), Harlan Sprague Dawley, Indianapolis, USA) weighing 2.5–3.5 kg were irradiated by heavy carbon ions using a 290 MeV/nucleon 6-cm spread-out Bragg-peak (SOBP) carbon-ion beam (10 cm in diameter) of the Heavy-Ion Medical Accelerator in Chiba (HIMAC) at the National Institute of Radiological Science, Chiba, Japan. The relationship between the dose rate, LET, and water-equivalent residual range of the beams is shown in Fig. 1. Each cat was anesthetized with an intramuscular injection of ketamine (5 mg/kg Ketalar 50^{TM}, Sankyo, Tokyo). The left cerebral hemispheres of each of two cats were irradiated once from the front (the transverse and vertical widths were 3 cm and 2.5 cm, respectively) with doses of 15, 20, 30, and 35–40 Gy with the orbitomeatal line tilted by 30° by turning the face downward. Fig. 1 shows that the position of each cat was adjusted such that a Bragg peak was located at 2.5 cm under the parietal tip of the skull and 6.0 cm from the face (arrow in Fig. 1). An additional cat was used as a nonirradiated control.

Twelve months later, these cats were anesthetized with ketamine and killed by intravenous infusion of 5 ml of sodium pentobarbital solution (Nembutal, Dainippon Pharmaceutical Co., Osaka). They were then perfused with 2% glutaraldehyde solution from the left cardiac ventricle for 30 min under a pressure of 60 mmHg. Most of the viscera was weighed and examined histologically. From the brain removed from the skull, 0.5-mm-thick strips including the total cortical layers and subcortical white matter of the bilateral suprasylvian gyrus, the left of which was irradiated, were first resected for electron-microscopic examination of the capillary density. Then, the whole brain was coronally dissected, and these slices were embedded in paraffin and sectioned at a thickness of 5 μm. These sections were stained with hematoxylin-eosin (HE), Kluever-Barrera (KB), Bodian, periodic acid methenamine (PAM)-KB, and elastica-Masson, and immunohistochemically stained with an antibody to glial fibrillary acidic protein (GFAP) (polyclonal antibovine GFAP, DAKO, Denmark; ×200) after boiling the sections in 10 mM citrate buffer, pH 6.0, for 15 min. A 1-cm-thick coronal slice including the bilateral marginal and the suprasylvian and ectosylvian gyri of each cat was completely serially sectioned; every fifth section was stained with PAM-KB, and several sections were immunohistochemically stained with antibodies to smooth muscle α-actin (monoclonal mouse antibody to human α-smooth-muscle actin, DAKO, Denmark) to differentiate a small artery from a vein, and albumine (polyclonal anticat albumin, Bethyl Laboratories, USA; ×20,000) for the detection of any disturbance of the blood–brain barrier. In a cat irradiated with 35 Gy that exhibited prominent vascular changes and a large cavitation of the deep white matter, these serial sections were reconstructed so as to investigate the mutual spatial relationship of the parenchymal and vascular changes, such as the existence of fibrinoid necroses, thrombi, damage to the medial smooth muscle cells (SMCs) of the arteries, and arteriovenous shunt; 18 medullary arteries and two neighboring veins in serial sections stained with PAM-KB in the irradiated cerebral white matter were traced from the penetrating level at the cortical surface to the precapillary level of these vessels on clear polyester films (OHP films) under a microscope (×5–10 magnification), and the total courses that were included in a thickness of 60–2,000 μm were reconstructed.

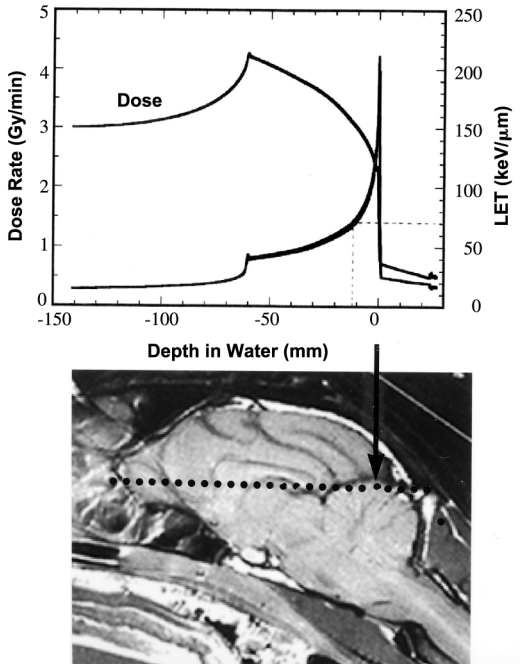

Fig. 1. Relationship between the dose rate, linear energy transger (LET), and water-equivalent residual range of a 290 MeV/nucleon 6-cm SOBP carbon-ion beam of 10 cm diameter at the HIMAC. The arrow indicates the position of a Bragg-peak. The dotted line is the orbitomeatal line.

For a morphometric examination of the capillary density of the suprasylvian gyrus, the cortex in the resected each strip was divided along the midline into superficial and deep layers. These cortical and subcortical- white matter specimens

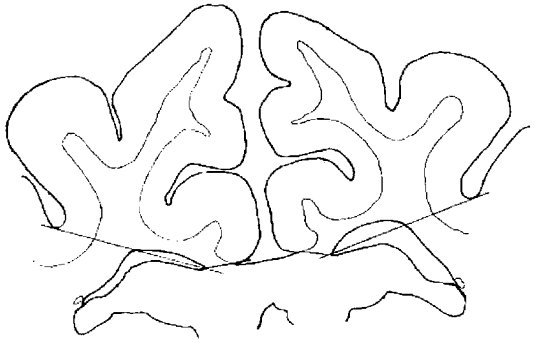

Fig. 2. Morphometrically measured area of the bilateral marginal and suprasylvian gyri. The areas of the bilateral sides of the cortex and white matter above these lines were measured separately.

were embedded in an Epon 812 mixture (TAAB, UK), and the thin sections were stained with lead and uranyl acetate, and examined using an electron microscope (H-600, Hitachi, Japan). Capillaries within a 147 × 147 μm square mesh were counted in 20–40 meshes for each specimen from a cat. These numbers were compared between the left and right cortices in each cat, and between the irradiation doses. Here, a capillary was defined as a vessel lined with endothelia and a basement membrane without SMCs and perivascular spaces.

The volume of the cortex (*C*) and white matter (*W*), and the ratio thereof (*W*/*C*) in the bilateral marginal and suprasylvian gyri, were measured in serial sections; contours of the cortex of 12–20 sections stained with KB were traced on papers, and the areas of the cortex and white matter above a line binding the internal edge of the lateral ventricle to the bottom of the suprasylvian sulcus (Fig. 2) were measured by weighing each cut portion.

The capillary density of the suprasylvian gyrus, and *C*, *W*, and *W*/*C* for the marginal and suprasylvian gyri were compared between the left (irradiated) and right (nonirradiated) by a Student's *t*-test.

This experiment was approved by the Animal Care and Use Committee of Tokyo Medical & Dental University (Approval No.0001009).

RESULTS

Neurological findings and cutaneous changes at the irradiated parts between the irradiation and sacrifice

Neurologically, abnormal signs in the gait or movement of the extremities were not recognized after irradiation, the food intake was generally normal, the body weight was not reduced, although one cat irradiated with 20 Gy vomited twice 4 and 5 months after irradiation. A few weeks after irradiation, hairs of the cranial skin had fallen out at the irradiated left parietal region of all cats, and then the skin became ulcerated. Such ulceration was associated with exposure of the cranial bone with its tiny defects in cats irradiated with doses of more than 30 Gy (Fig. 3A), which continued until sacrifice. Hematopoietic tissue of the bone marrow in the irradiated cranial bone disappeared at the time of sacrifice. However, acute meningitis or general infection was not detected at the autopsy.

Neuropathological findings

Macroscopically, the brain and the viscera were not remarkable, except for the above-described changes of the cranial bone.

Histologically, as shown in Table 1, slight cytoplasmic swelling of the astrocytes in the irradiated white matter was the sole pathological finding in two cats irradiated with 15 Gy. In two cats irradiated with 20 Gy, this was accompanied by a slight dilatation of small vessels. The irradiated cerebral cortex was not remarkable. In two cats irradiated with 30 Gy, the dilatation of small vessels became more prominent (Fig. 3B), exhibiting a diffuse thickening of the wall due to the thickened basement membrane and adventitial fibrosis, a few foci of perivascular cuffing of mononuclear cells, and a slight-to-moderate loosening with tiny cavitations in the white matter (Fig. 3C). These cavities were scattered in the deep white matter (arrowheads of Fig. 3C), and included floccular and grobular debris; the margin was irregular, and vascular proliferation in these cavities or fibrous gliosis surrounding these cavities was absent (Fig. 3D, left and right). Swollen astrocytes and their processes were scattered in and around these cavities. Albumin was deposited on the floccular contents and inner surfaces of these cavities (Fig. 3D, middle), and sometimes a few myelinated fibers or swollen axons or calcospherites were present in these cavities, in addition to a few macrophages. Some of these cavities contained a vein in the center (Fig. 3E). The irradiated cortex showed a slight swelling of perivascular astrocytes. In a cat irradiated with 35 Gy, these changes in the white matter were definitely more

Table 1. Pathological findings of the left cerebral hemisphere in 1 year after irradiation.

Dose	Cerebral white matter				Cortex
	Astro-swell	Vas-Dil/ Mural-t	PC	Loosening/ Cavity	
15 Gy	+	–/–	–	–/–	–
15 Gy	+	–/–	–	–/–	–
20 Gy	+	+/–	–	–/–	–
20 Gy	+	+/–	–	–/–	–
30 Gy	++	++/+	+	+/+	+*
30 Gy	+++	+++/++	++	++/+	+*
35 Gy	+++	+++/+++	++	+++/++	++#

Astro-swell: astrocytic swelling, Vas-dil: vascular dilatation, Mural-t:mural thickening, PC: perivascular cuffing of inflammatory mononuclear cells, +: slight degree, ++: moderate degree, +++: severe degree, +*: slight vascular dilatation and swelling of astrocytic processes, ++#: positive albumin deposition in astrocytes.

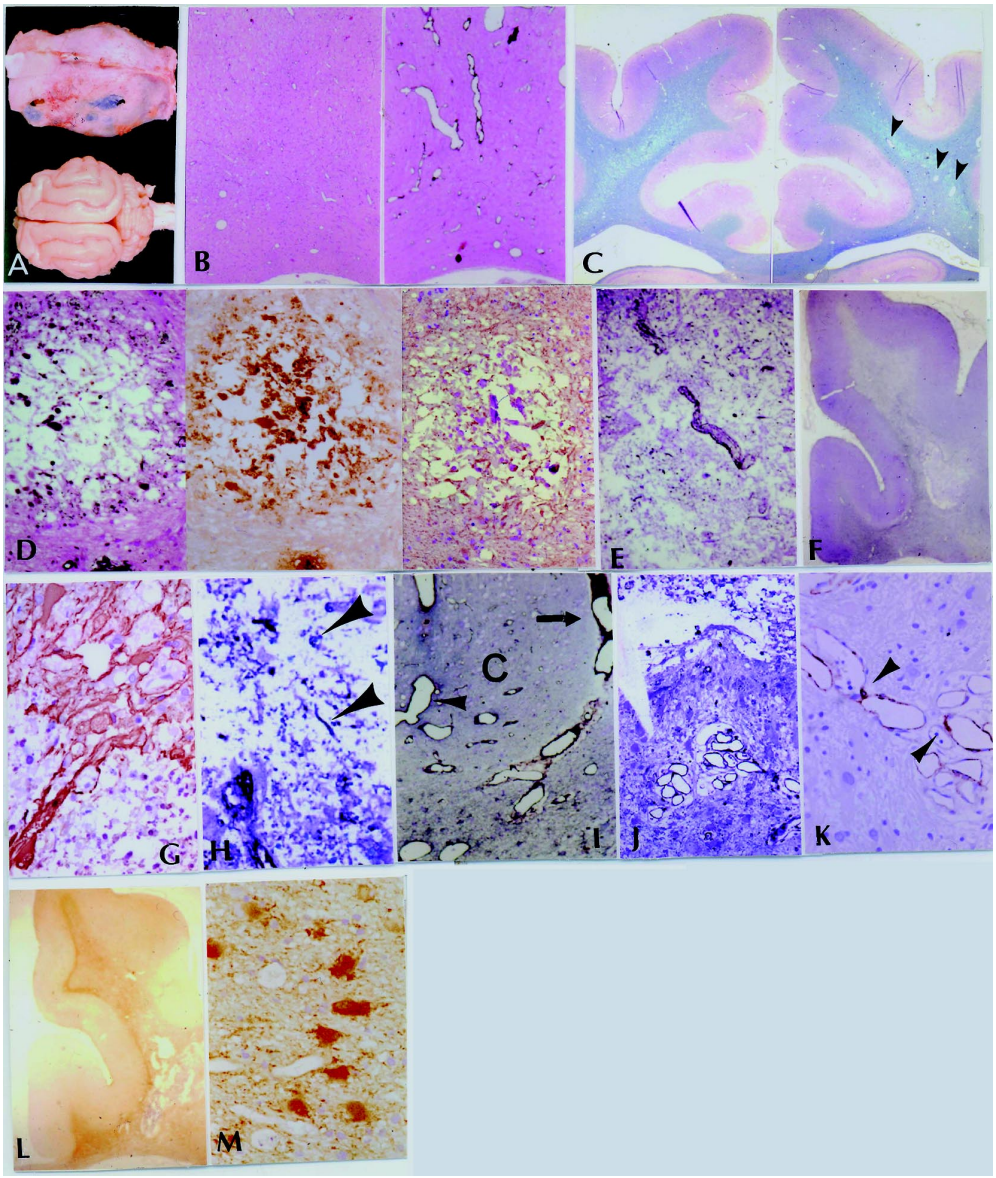

Fig. 3. Histological findings. A: The cranium and brain of a cat irradiated with 30 Gy. The bone of the left parietal portion became thin and perforated, but the brain was not remarkable macroscopically. B: Vascular dilatation with thickening of the basement membrane of the deep white matter of the left irradiated hemisphere (the right) of a cat irradiated with 30 Gy as compared with the right hemisphere (the left). ×15. C: The white matter of the left hemisphere (the right) of a cat irradiated with 30 Gy presents diffuse myelin pallor with a few tiny cavities (arrowheads) in the deep portion: the left is the right hemisphere (PAM-KB staining). D: A tiny cavity in the deep white matter of a cat irradiated with 30 Gy. The left: In the cavity unstained floccular and globular material and calcospherites are present, and in the wall a few macrophages containing PAM-positive granules are seen (PAM-HE stain). ×60. The middle: Albumin deposition in and around the cavity of D, left. ×60. The right: Astrocytic processes increase slightly in and around the cavity, but fibrous gliosis is absent (GFAP). ×60. E: A small vein is located in the center of a tiny cavity of a cat irradiated with 35 Gy. (PAM-HE). ×30. F: Diffuse myelin pallor with an irregularly shaped large cavity of the white matter of a cat irradiated with 35 Gy. G: Around the large cavity of Fig. 3F, astrocytes and fibrillary bundles are scattered, and protrude from the wall into the cavity without surrounding the cavity (GFAP). ×60. H: Several macrophages and fragments of myelinated fibers (arrowheads) float in the large cavity of Fig. 3F. Several swollen astrocytes are scattered in the wall (PAM-KB). ×60. I: A dilated medullary artery (arrow) locates from the cortex (C) to the white matter, and a dilated vein (arrowhead) locates from the subcortical white matter into the cortex (PAM-KB). ×30. J: Conglomerates of dilated vessels in the wall of a large cavity of a cat irradiated with 35 Gy (PAM-KB). ×60. K: Dilated small vessels of a vascular conglomerate of Fig. 3J have smooth muscle cells (arrowheads) in the wall. α-smooth muscle cell actin immunostaining, ×120. L: Diffuse albumin deposition in the white matter of the left cerebral hemisphere of a cat irradiated with 35 Gy. The deposition is accentuated in the subcortical white matter. (albumin immunostaining). M: Prominent albumin deposition in the swollen astrocytic cytoplasma and processes in the left cerebral white matter of a cat irradiated with 35 Gy. ×60.

prominent. Additionally, a diffuse, but irregularly accentuated, loosening of the subcortical and deep white matter of the supraventricular region occurred (Fig. 3F), which involved the subcortical U-fibers at the marginal gyrus. In the loosened white matter, most axons and oligodendroglias were well preserved, but a few tiny cavities and a large irregularly shaped cavity were present in the deep white matter (Fig. 3F). Swollen astrocytes and many fine glial bundles protruded from the wall into those cavities without surrounding the wall (Fig. 3G). Some myelinated axons floated in these cavities (Fig. 3H). Prominent dilatations of veins and capillaries were also noticeable in the loosened white matter (Fig. 3I), and a few conglomerates of dilated vessels were found near a few large cavities (Fig. 3J). The reconstruction of 18 medullary arteries and the two neighboring large veins in the serial sections of a cat irradiated with 35 Gy revealed that these dilated vessels comprised arteries, veins, and capillaries, and that no fresh or organized thrombi, fibrinoid degeneration, any arteriovenous shunts, or SMC damage of the arterial media was present there; the dilatation of these arteries began in the deep cortical layer or subcortical white matter, and connected to dilatated capillary-like vessels, which exhibited perivascular spaces different from those of true capillaries. The dilated vessels of these conglomerates had sparsely SMCs in the wall (Fig. 3K) and, therefore, these were small arteries. Direct continuity from these dilated small arteries to the dilated small veins (arteriovenous shunt) was not detected. From the level of these dilated small veins to the cortical surface vein, the veins were continuously and prominently dilated. The cortex was well preserved, and an extension of the cavities in the white matter into the cortex was absent. In a cat irradiated with 40 Gy, irregular loosening with astrocytic swelling of the subcortical white matter of the marginal and suprasylvian gyri was present, but the deep white matter was well preserved, and cavities were absent.

Albumin exudation was not detected in two cats irradiated with 15 Gy and in one cat irradiated with 20 Gy. In another cat irradiated with 20 Gy, swollen astrocytes, endothelia of small vessels, and adventitia of large vessels in the left white matter were positive for albumin. In two cats irradiated with 30 Gy, the white matter of the left was diffusely albumin-positive, and astrocytes, endothelia of small and large vessels, and arterial and venous adventitia were also positive. In a cat irradiated with 35 Gy, albumin deposition was especially prominent at the subcortical U-fibers (Fig. 3L and M), and also diffusely positive in the cortex. It was positive not only in the astrocytes, but also in neuropils and neuronal cytoplasma in the cortex. In a cat irradiated with 40 Gy, albumin was not detected in the left white matter, except for in a few astrocytes around the veins, and was positive irregularly around neurons in the cortex. From the above-described histological findings, it was considered that this case was irradiated only to the superficial region of the left cerebral hemisphere, such that the deep white matter was not irradiated.

Table 2. **Table 2.**Capillary density of the suprasylvian gyrus: Comparison between the left (irradiated) and right (nonirradiated) sides. Mean of number of capillaries and standard error/mesh of 147 × 147 μm. ( ): number of counted meshes.

Dose	Cortex		White matter
	Superficial layer	Deep layer	
30 Gy			
1. The left	3.65 ± 0.31 (20)	2.35 ± 0.41 (14)**	1.40 ± 0.18 (35)
The right	4.09 ± 0.37 (22)	3.19 ± 0.17 (46)	1.71 ± 0.16 (52)
2. The left	4.40 ± 0.19 (56)	3.67 ± 0.29 (37)*	1.07 ± 0.10 (83)##
The right	5.05 ± 0.29 (40)	4.76 ± 0.28 (38)	1.50 ± 0.11 (84)
30 Gy			
1. The left	5.73 ± 0.43 (30)	2.32 ± 0.20 (34)#	1.67 ± 0.15 (43)
The right	6.12 ± 0.37 (40)	4.56 ± 0.28 (32)	1.56 ± 0.18 (39)
2. The left	4.72 ± 0.25 (65)#	3.35 ± 0.30 (31)#	0.02 ± 0.02 (40)#
The right	6.65 ± 0.32 (35)	5.43 ± 0.37 (30)	1.70 ± 0.19 (51)
35 Gy			
The left	5.83 ± 0.67 (12)	5.84 ± 0.42 (13)	1.74 ± 0.18 (31)
The right	6.70 ± 0.47 (10)	6.64 ± 0.67 (17)	1.88 ± 0.22 (27)
40 Gy			
The left	5.06 ± 0.41 (16)##	5.47 ± 0.28 (21)	0.67 ± 0.16 (28)#
The right	7.00 ± 0.40 (15)	5.70 ± 0.50 (17)	2.87 ± 0.21 (33)

*$p < 0.02$, **$p < 0.05$, #$p < 0.001$, ##$p < 0.005$.

Table 3. Volume of the cortex (C) and white matter (W), and ratio of the both (W/C) of the parietal region-Comparison between the left (irradiated) and right (nonirradiated) sides. (< or >: $p < 0.05$) (*n*: number of sections studied)

Dose	Total volume left:right	C left:right	W left:right	W/C left:right
15 Gy				
1 (*n* = 20)	<	<	>	>
2 (*n* = 20)	>	#	>	>
20 Gy				
1 (*n* = 20)	>	#	>	#
2 (*n* = 20)	>	>	>	>
30 Gy				
1 (*n* = 12)	#	#	>	>
35 Gy				
(*n* = 20)	#	<	>	>
40 Gy				
(*n* = 20)	#	#	>	>
Control				
(*n* = 20)	#	#	#	#

#$p > 0.05$.

Morphometric findings of capillary density and volume of the cortex and white matter

Table 2 presents the results of morphometric observations of the capillary density in the suprasylvian cortex and white matter of cats irradiated with more than 20 Gy. The density is here expressed as capillary numbers per mesh (147 × 147 μm), as observed under an electron microscope, and compared between the left (irradiated) and right (nonirradiated) sides. The capillary density of the deep cortical layer and white matter of the irradiated side was generally lower than that of the nonirradiated side, with the difference being statistically significant in some cats, whereas the nonirradiated control cat showed no difference between the two sides (data not shown).

Table 3 provides morphometric comparisons between *C*, *W*, and *W*/*C* for the left and right sides of the marginal and suprasylvian gyri. This shows that the volume difference between the left and right sides of the cortex was variable, but the white-matter volume of the left increased significantly in all cats irrespective of the radiation dose, and the increase in *W*/*C* on the left side was also significant in most cats.

DISCUSSION

The characteristics of the above-described heavy-ion-induced neuropathological changes of the white matter, such as loosening and cavity formation, and vascular changes of cats were the same as those of delayed radiation-induced myelopathy of rats.[1, 2] Some of these cavities included venous vessels in the center. A few myelinated fibers (some of which crossed these cavities) and a few macrophages were present on the walls of these cavities, and bundles of astrocytic processes protruded from the wall into these cavities. However, fibrous gliosis surrounding these cavities was not recognized. The pathological findings suggest that these cavities were caused not by infarction, but by long-standing edema around the veins and capillaries, which was dose dependent and diffusely, but irregularly, accentuated. Delayed encephalopathy induced by X-ray irradiation in humans presents severe exudative destruction (Plasmatische Infiltrationsnekrose: Scholz[4]) of the white matter also exclusively around the veins.[5] One of the morphometric findings from this study, that the volume of the white matter and volume ratio of the white matter to the cortex of the irradiated left hemisphere were generally larger than those of the nonirradiated right side, indicates that edema was still present 1 year after irradiation. This also supports the assumption of edema-induced destruction. The preferential involvement of the white matter in the case of either encephalopathy or myelopathy can be explained by the loose extracellular space (ECS) being different from the narrow and tight ECS of the cortex, and that the continuous vascular hyperpermeability inducing long-standing edema, which is evidenced by diffuse deposition of albumin in the irradiated white matter in our study, is the cardinal pathogenesis. Fibrous thickening of dilated vessels may be explained by reactive fibrosis and a thickening of the vascular basement membrane due to such continuous hyperpermeability.

What is the mechanism of the hyperpermeability in the irradiated white matter? It is already reported that edema or hyperpermeability occurs in white matter 12-14 weeks after a single X-ray irradiation of at least 25 Gy,[6] but the underlying mechanism is still unknown. Okada e*t al.*[3] demonstrated that EBA expression begins to decrease, or even disappear, at the capillaries and veins in the spinal white matter by 13 weeks after heavy-ion irradiation of 30 Gy in rats. This change becomes prominent at 15–17 weeks, just before the development of white matter destruction. In that study, a tight-junction-related molecule, ZO-1, was well preserved. It is highly possible that some endothelial dysfunction occurs after such a long latency. As a mechanism of radiation-induced blood-brain barrier (BBB), upregulation of vascular endothelial growth factor (VEGF) in astrocytes is proposed.[7] However, VEGF expression was very week in our experimental radiation myelopathy,[3] and it is not specific for irradiation. In addition, it is reported that gelatinase B and urokinase were elevated in the irradiated and necrotized portion in the case of astrocytoma, and that these enzymes may participate radiation injury.[8] However, it should be confirmed whether this finding is primary (direct effect of irradiation) or secondary to tissue injury. The biological mechanisms, therefore, are not conclusive, and should be investigated in the future.

Another problem is the pathogenesis of vascular dilatation.

Vascular dilatation (telangiectasia) in irradiated CNS is well known, and it is generally most prominent at least 1 year after irradiation.[9] Under several conditions, such as Binswanger disease,[10] amyloid angiopathy or cerebral autosomal dominant arteriopathy with infarcts, and leukoencephalopathy (CADASIL),[11] in which the cerebral white matter is diffusely and severely affected by edema-induced myelin loss and atrophy,[12] the severe vascular dilatation seen in delayed radiation-induced encephalopathy or myelopathy is usually absent. Therefore, it is radiation-specific and the underlying mechanisms might be (1) radiation-induced weakening of the vascular envelope or changes in the surrounding tissue, (2) stagnation or altered flow in certain capillaries, (3) proliferation of the endothelium resulting in an increased total blood vessel surface area due to an accumulation of angiogenic factors, and/or (4) microvascular shunting or degeneration of arterial SMCs.[13] Vascular dilatation occurred in the veins, arteries, and capillaries in the parenchyma of the irradiated cerebral hemisphere in this experiment, and was absent or only very slight in cats irradiated with 15 or 20 Gy, but became prominent in cats irradiated with 30 Gy or 35 Gy. This dose dependency in the extent of the vascular dilatation was evident also in the mean cross-sectional area in the lateral funiculus of heavy-ion-induced delayed radiation myelopathy in rats, and the extent of the dilatation of each vessel was negatively correlated with the decreases in the vascular numbers in rats.[2] In a cat irradiated with 40 Gy in our study, vascular dilatation and cavity formation of the cerebral white matter were not present, although the cerebral white matter of the left side was significantly swollen and the capillary density of the subcortical white matter was significantly depleted. Albumin deposition was present in this case in the perineuronal neuropils and perivascular astrocytes in the cortex, but it was restricted in the perivascular astrocytes of the subcortical white matter, and absent in the deep white matter. Therefore, it is reasonable to suppose that in this cat only the superficial region of the left cerebral hemisphere received radiation because of insufficient tilting down of the face, resulting in placing the deep white matter outside the irradiation field. If this assumption is correct, the vascular dilatation may not only be dose-dependent, but also dependent on the irradiated tissue volume. Moreover, the capillary density in the deep cortex and subcortical white matter of the irradiated left hemisphere of most cats decreased, although this effect was not dose dependent. This decrease of the capillary density can be explained by capillary destruction due to irradiation or capillary compression due to edema, or by both mechanisms. On the other hand, the number of vessels in the lateral funiculus of the spinal cord of rats irradiated with heavy ions decreased dose-dependently. Therefore, there is the possibility that the decrease of the vascular bed induces arterial and venous stagnation, or a break-through (arteriovenous shunt) between the arterial and venous sides, resulting in vascular dilatation. In this study, however, reconstruction of the 18 dilated cerebral medullary arteries and the two neighboring veins using serial sections did not result in the detection of any arteriovenous shunt and damage to arterial SMCs. Moreover, it is reported that the regional blood flow and vascular volume decrease (the maximum decrease is in 3 weeks after irradiation) in lesions associated with interstitial radiation-induced encephalopathy, but that the vascular volume then increases in 6 weeks.[14] These authors proposed that the increase of the vascular volume in the necrotic lesion is due to neovascularization, and that the necrosis is due to ischemia. This experiment could not support their proposals. Thus, in addition to a factor of vascular loss by irradiation, hemoconcentration by hyperpermeability in the vascurature in the irradiated white matter seems to be a very important factor for vascular stagnation and following dilatation. However, this issue requires further examination because the present study lacks evidence of hemoconcentration.

ACKNOWLEDGEMENTS

This investigation was supported by the Research Project with Heavy Ions at the National Institute of Radiation Sciences-Heavy-Ion Medical Accelerator in Chiba (NIRS-HIMAC).

REFERENCES

1. Miyagawa, H., Yokofujita, J., Okeda, R. and Kuroiwa, T. (1996) Pathogenesis of delayed radiation injury in the rat spinal cord after X-ray irradiation. Neuropathology **16**: 126–132.
2. Okada, S., Okeda, R., Matsushita, S. and Kawano, A. (1998) Histopathological and morphometrical study of the late effects of heavy-ion irradiation on the spinal cord of the rat. Radiat. Res. **150**: 304–315.
3. Okada, S., Okeda, R., Matsushita, S. and Kawano, A. (1998) Immunohistochemical changes of the blood-brain barrier in rat spinal cord after heavy-ion irradiation. Neuropathology **18**: 188–198.
4. Scholz, W.and Hsue, Y.K. (1938) Late damage from roentgen irradiation of the human brain. Arch. Neurol. Psychiat. **40**: 928–936.
5. Okada, S. and Okeda, R. (2001) Pathology of radiation myelopathy (review article). Neuropathology **21**: 247–265.
6. Stewart, P.A., Vinters, H.V. and Wong, C.S. (1995) Blood-spinal cord barrier function and morphometry after single doses of x-rays in rat spinal cord. Int. J. Radiat. Oncol. Biol. Phys. **32**: 703–711.
7. Tsao, M.N., Li, Y.Q., Lu, G., Xu, Y. and Wong, C.S. (1999) Upregulation of vascular endothelial growth factor is associated with radiation-induced blood-brain barrier breakdown. J. Neuropathol. Exp. Nerurol. **58**: 1051–1060.
8. Adair, J.C., Baldwin, N., Komfeld, M. and Rosenberg, G.A. (1999) Radiation-induced blood-brain barrier damage in astrocytoma: relation to elevated gelatinase B and urokinase. J. Neurooncol. **44**: 283–289.
9. Reinhold, H.S. and Hopewell, J. W. (1980) Late changes in

the architecture of blood vessels of the rat brain after irradiation. Br. J. Radiol. **53**: 693–696.
10. Tanoi, Y., Okeda, R. and Budka, H. (2000) Binswanger's encephalopathy: serial sections and morphometry of the cerebral arteries. Acta Neuropathol. **100**: 347–355.
11. Okeda, R., Arima, K. and Kawai, M. (2002) Arterial changes in cerebral autosomal dominant arteriopathy with subcortical infarcts and leukoencephalopathy (CADASIL) in relation to pathogenesis of diffuse myelin loss of cerebral white matter. Examination of cerebral medullary arteriesby reconstruction o serial sections of an autopsy case. Stroke **33**: 2565–2569.
12. Feigin, I. and Popper, N. (1963) Neuropathological changes late in cerebral edema: the relationship to trauma, hypertensive disease and Binswanger's encephalopathy. J. Neuropathol. Exp. Neurol. **22**: 500–511.
13. Okeda, R. and Shibata, T. (1973) Radiation encephalopathy – an autopsy case and some comments on the pathogenesis of delayed radionecrosis of central nervous system. Acta Pathol. Jpn. **23**: 867–883.
14. Gobbel, G.T., Seilhan, T.M. and Fike, J.R. (1992) Cerebrovascular response after interstitial irradiation. Radiat. Res. **130**: 236–240.

Received on May 19, 2003
1st Revision on September 16, 2003
Accepted on September 16, 2003